Second Conference on Smart Monitoring,
Assessment and Rehabilitation of Civil Structures

SMAR 2013

Constitutive Laws of FRP-Reinforced Concrete Element under Pure Shear

G. Yang[1], M. Zomorodian[2], A. Belarbi[3], A. Ayoub[4], and B. Acun[5]

[12] PhD candidate, University of Houston, Houston, US
[3] Professor and Department Chair, University of Houston, Houston, US
[4] Associate Professor, University of Houston, Houston, US
[5] Postdoc Researcher, University of Houston, Houston, US

ABSTRACT: Fiber Reinforced Polymer (FRP) has been widely used in strengthening the civil engineering structures for decades. Well established analytical procedures can be applied to design strengthening systems for beams and columns in flexure. However, the study on shear behavior is still on a developing stage. This paper presents the results of an on-going project. It aims to develop a rational model to evaluate the behavior of the FRP strengthened reinforced concrete element subjected to pure shear. A series of large-scale tests were conducted using the Universal Panel Tester at the University of Houston (UH). The UH research group proposed several analytical models earlier to predict the shear behavior of RC members, of which the most recent one is the Softening Membrane Model (SMM). To take into account the FRP in strengthening, a new SMM-FRP is developed and verified by experimental results. The SMM-FRP shows good agreement with the current test results.

1 INTRODUCTION

In the past three decades, several analytical models were proposed to predict the shear behavior of the reinforced concrete element. The concept of “smeared” stress/strain was used to overcome the complexity of the post-cracking behavior of RC elements. To build up the new constitutive laws, several tests were conducted by Vecchio & Collins (1982, 1986), Belarbi & Hsu (1994, 1995), Zhang & Hsu (1998), Pang & Hsu (1996), Zhu & Hsu (2002), and Wang & Hsu (2006). The most recent model, Softening Membrane Model (SMM), is proposed by Zhu & Hsu (2002). The SMM has been proven to predict the whole stress-strain curve of the RC member under pure shear reasonable good. The SMM provides some basic knowledge of the shear behavior of RC elements; however, it cannot be applied directly to the reinforced concrete members strengthened with FRP (FRP-RC element). The FRP substantially affects the crack patterns due to bond between the concrete and applied FRP at surface and consequently the failure modes of the RC members. Moslehy (2010) conducted 12 tests on panel specimens to evaluate the variation of the softening coefficient for FRP RC element. His results showed that the softening coefficient was increased by the confinement of the externally bonded FRP sheets. Test data also show an increase of the strength on the post-cracking stage compared with the RC element without FRP. By utilizing the new constitutive laws proposed by Moslehy (2010), a new SMM-FRP is developed in this study.

2 TEST PROGRAM

2.1 Universal Panel Tester

The Universal Panel Tester (UPT) was constructed at the University of Houston in 1986. It is custom-designed to perform biaxial and/or tri-axial tests on reinforced concrete panels (Figure 1). With its unique properties, the UPT is capable of testing full-scale panels with dimensions up to 1.4x1.4 m, and thickness up to 406 mm. The panel specimens, in general, represent an element extracted from real-scale reinforced concrete structures, such as bridge girders, shell roofs, nuclear containment structures, concrete offshore platforms or high-rise shear walls. The UPT is composed of a high strength steel reaction frame, a set of hydraulic cylinders (40 in-plane and 10 out-of-plane) that are used to apply forces on panel specimens and a 35 MPa hydraulic pump unit with complex series of valves and hoses to provide desired level of load. Each of the hydraulic cylinders provides a load up to 1110 kN in compression and 890 kN in tension. The hydraulic cylinders can be controlled manually (mainly at preparation stage) or automatically (at testing). The tests can be conducted both in load controlled or displacement controlled manner. A servo-control system, containing 10 servo controllers which are connected to 10 hydraulic manifolds, ensures uniform loading on each side. Pressure transducers that are installed in each manifold monitor the pressure and provide feedback to the servo controllers. The servo controller takes commands from a programmer, compares it with the feedback, and sends modified commands to servo valve accordingly. The feedback could be pressure measured by the transducer (load control mode) or strain measured from LVDT (strain control mode).

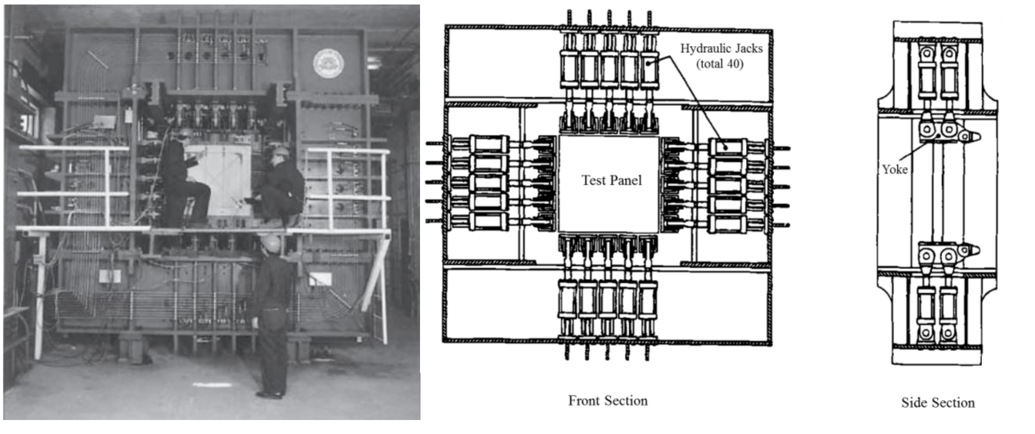

Figure 1. Illustration of load application by in plane hydraulic jacks, Hsu et al. (1995).

2.2 Test Specimen

The prototype test specimens are square RC panels with approximately 1.4m dimension and 178 mm thickness. The concrete compressive strength of the specimens is around 48 MPa. Two different steel arrangements can be used for different test purposes (Figure 2). The first arrangement is for the softening tests, in which the biaxial load is applied sequentially. The second one is for pure shear testing, in which equal tensile and compressive loads are applied in the horizontal and vertical directions respectively, in order to create a pure shear condition at an angle of 45°. Earlier, Mohsley (2010) tested 12 panels to study the softening coefficient using the first kind of steel arrangement. The specimens were strengthened with horizontally applied FRP sheets. The tensile load was also applied horizontally, followed by the compressive load in the vertical direction until the concrete crushing. Some of his experimental results were utilized in this study for derivation of the constitutive modeling of SMM-FRP.

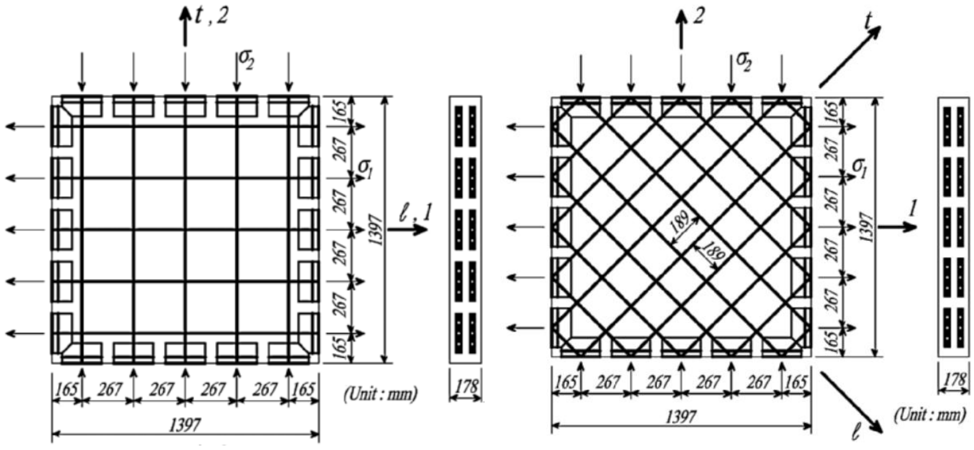

Figure 2. Dimensions and coordinates of the tested panels.

Two RC panel elements strengthened with 1mm thick FRP sheets (FRP-RC element) and with the latter reinforcement arrangement are tested under pure shear. The FRP-RC element represents a cutoff piece from a FRP strengthened reinforced concrete beam under shear (Figure 3). The applied FRP strips were 144 mm wide with a spacing of 189 mm center to center. The sheets were wrapped around the bottom and the right side of the panel to simulate the U-wrap scheme, as shown in Figure 3. The other end of the FRP sheet was cut right at the edge of the top and left side of the panel. An anchorage system is used for one of the specimens on these ends to simulate the anchor applications in beams for FRP strengthening. Other parameters of these two specimens are identical.

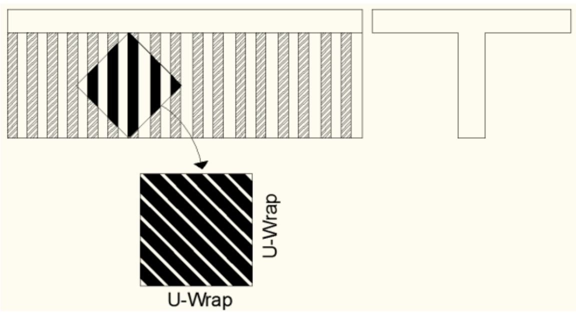

Figure 3. The T-Beam idealized as an assemblage of membrane elements.

Standard material tests were conducted in the materials laboratory at the UH for concrete and steel and the results are listed in Table 1 below. Material properties of FRP are taken from the specifications of the producer.

Table 1. Material properties of the panel

Concrete	f'_c=48.6 MPa	E_c=27020 MPa	ε_{cr}=0.00008
Steel rebar	ρ_l=ρ_t=0.756%	E_s=212700 MPa	f_y=414 MPa
FRP	ρ_f=0.871%	E_f=72390 MPa	f_u=876 MPa

The two tested panel specimens, namely F2S1 and F2S2, exhibited different failure modes. The first panel specimen, F2S1, failed due to premature debonding of FRP sheets and subsequently the crushing of concrete; however for the second specimen, F2S2, the failure mode was the rupture of FRP and failure of anchors. The FRP anchors used in strengthening of second specimen were made by a bundle of the carbon fiber same as the FRP sheets to provide compatibility between the materials used. After saturating the FRP anchor into epoxy resin, one end of the anchor was inserted through a pre-drilled hole on the concrete surface, and the fiber on the other end was then spread on top of the FRP sheet. The details of the application of anchorage system and tests results can be found elsewhere (Zomorodian et al, 2013).

3 THEORY OF SMM-FRP

3.1 Constitutive law for concrete in tension

In SMM-FRP, the constitutive law of concrete in tension was proposed by Belarbi & Hsu (1995):

$$\sigma_1^c = E_c\bar{\varepsilon}_1 \qquad \bar{\varepsilon}_1 < \varepsilon_{cr} = 0.00008 \tag{1}$$

$$\sigma_1^c = f_{cr}\left(\frac{\varepsilon_{cr}}{\bar{\varepsilon}_1}\right)^{0.4} \qquad \bar{\varepsilon}_1 \geq \varepsilon_{cr} = 0.00008 \tag{2}$$

The notations of above and following equations are presented in Notations section.

In the softening test of the FRP-RC element (Moshley, 2010), horizontal tensile load was applied first. The FRP contributed to the resistance as a tension member and functioned in conjunction with the RC element. The theoretical stress and strain distributions between cracks are shown in Figure 4.

The longitudinal equilibrium of forces at any section x between the two cracks leads to:

$$P = A_s\sigma_s(x) + A_f\sigma_f(x) + A_c\sigma_c(x) \tag{3}$$

The tensile stress-strain relationship of concrete actually relates the smeared stress and smeared strain. The smeared strain includes not only the concrete strain but also the crack width. Hence, the smeared strain stands for the smeared strain in the steel/FRP or the smeared strain in the concrete including cracks. In the tests, this strain could be measured by LVDTs.

The average stress of the steel and FRP can be obtained by;

$$\sigma_s = \frac{1}{L}\int_0^L \sigma_s(x)dx \qquad \sigma_f = \frac{1}{L}\int_0^L \sigma_f(x)dx \tag{4}$$

Since the concrete cracked at a lower level of strain, the steel and FRP can be treated as elastic materials:

$$\sigma_s = E_s\frac{1}{L}\int_0^L \varepsilon_s(x)dx \qquad \sigma_f = E_f\frac{1}{L}\int_0^L \varepsilon_f(x)dx \tag{5}$$

The definition of the smeared strain is:

$$\bar{\varepsilon}_1 = \frac{1}{L}\int_0^L \varepsilon_s(x)dx = \frac{1}{L}\int_0^L \varepsilon_f(x)dx \tag{6}$$

Hence, the equation (1) becomes:

$$P = A_sE_s\bar{\varepsilon}_1 + A_fE_f\bar{\varepsilon}_1 + A_c\sigma_c(x) \tag{7}$$

Defining the steel ratio and FRP ratio as;

$$\rho_s = \frac{A_s}{A_c} \qquad \rho_f = \frac{A_f}{A_c} \tag{8}$$

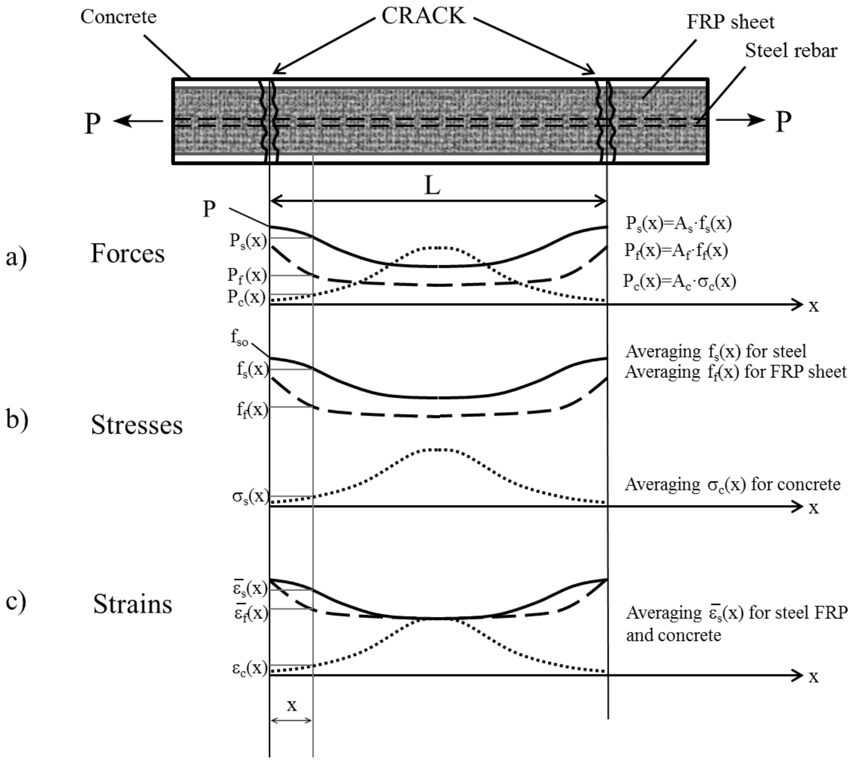

Figure 4. Force, stresses and strains between two cracks.

The equation becomes:

$$\sigma_c = \frac{P}{A_c} - \rho_s E_s \bar{\varepsilon}_1 - \rho_f E_f \bar{\varepsilon}_1 \tag{9}$$

The variables on Right Hand Side are known, so the smeared stress can be calculated accordingly (Figure 5). The available test data indicates that the strength of FRP-RC element at post-cracking stage is higher than that of the RC element. Hence, a new model is proposed based on Belarbi (1995) model. For elastic portion, Belarbi (1995) model is used as is and for post peak behavior a new formulation based on linear regression analysis is derived as follows:

$$\sigma_1^c = E_c \bar{\varepsilon}_1 \qquad \bar{\varepsilon}_1 < \varepsilon_{cr} = 0.00008 \tag{10}$$

$$\sigma_1^c = -425 * (\bar{\varepsilon}_1 - 0.00008) + 1, \quad 0.00008 \leq \bar{\varepsilon}_1 < 0.0015 \tag{11}$$

$$\sigma_1^c = E_c \bar{\varepsilon}_1 \qquad \bar{\varepsilon}_1 \geq 0.0015 \tag{12}$$

3.2 Softening coefficient

Moslehy (2010) proposed an equation for calculating the softening coefficient for FRP-RC element. This coefficient is applied for modifying the constitute law in compression. The softening coefficient is defined as:

$$\zeta = \left(\frac{5.8}{\sqrt{f'_c(\mathrm{MPa})}} \leq 0.9\right)\left(\frac{1}{\sqrt{1+400\bar{\varepsilon}_1}}\right)\left(1 - \frac{|\beta|}{24^0}\right) f(\mathrm{FRP}) \tag{13}$$

$$f(\mathrm{FRP}) = \left(1 + \frac{(16.785)E_f(\mathrm{MPa})\bar{\varepsilon}_1 (T_{FRP}(\mathrm{mm}))^{\frac{2}{3}}}{10^6}\right)(1.12 - 16\bar{\varepsilon}_1) \tag{14}$$

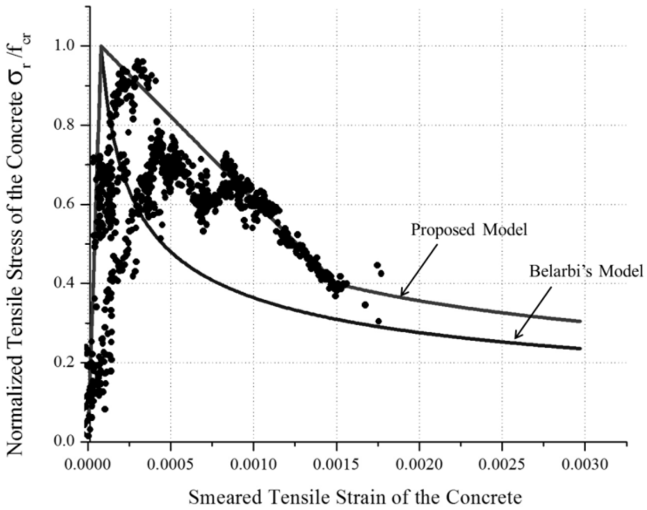

Figure 5. Tensile stress and strain curve for concrete.

3.3 *Stress equilibrium*

The stress in the FRP strip was considered similar to the steel reinforcement. The stress equilibrium proposed by Pang and Hsu (1996) is modified and a new term is added to tensile stress to take into account the contribution of the FRP sheets:

$$\sigma_l = \sigma_1^c \cos^2\alpha_1 + \sigma_2^c \sin^2\alpha_1 - \tau_{12}^c 2\sin\alpha_1\cos\alpha_1 + \rho_l f_l \quad (15)$$

$$\sigma_t = \sigma_1^c \sin^2\alpha_1 + \sigma_2^c \cos^2\alpha_1 + \tau_{12}^c 2\sin\alpha_1\cos\alpha_1 + \rho_t f_t + \rho_f f_f \quad (16)$$

$$\tau_{lt} = (\sigma_1^c - \sigma_2^c)\sin\alpha_1\cos\alpha_1 + \tau_{12}^c(\cos^2\alpha_1 - \sin^2\alpha_1) \quad (17)$$

3.4 *Comparison between the test data and SMM-FRP*

With these three modifications, the new SMM-FRP was developed. The details of all equations and the solution algorithm are presented in Yang et al. (2013). By solving all the equations, the shear stress and strain curve can be obtained. Comparison between the analytical prediction and the experimental results is presented in Figure 6. The figure shows good agreement between the results in cracking, yielding and peak points. Right after the cracking, the curve tends to be a plateau instead of a sudden decrease, this is due to the modified constitutive law of the concrete in tension. In the post-yielding portion, this effect was found to be insignificant, and the analytical model overestimated the stiffness at the post-yielding stage. The difference between the analytical and experimental results at ultimate state is around 8%. This could be caused by the large strain in the FRP after yielding of steel reinforcement, followed by a loss of bond strength between the FRP and concrete. The results of panel F2S1 is also shown in the same plot however, this panel failed by premature debonding of FRP sheets.

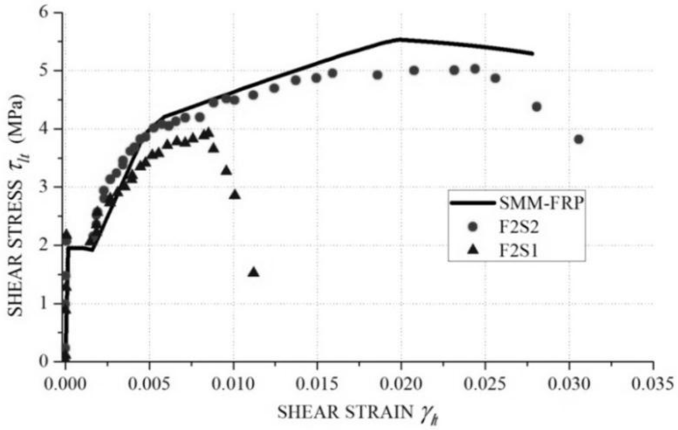

Figure 6. Comparison between the experimental and the analytical results of F2S1&F2S2.

4 CONCLUSIONS

From the result of this study, the following conclusions can be drawn:

- In the equilibrium equations of SMM-FRP, the FRP sheet can be treated similarly as the steel reinforcement. However, the interaction between the FRP and concrete can affect their constitutive laws. In this study, this effect was mainly considered on the softening coefficient and the tension of the concrete. By applying the FRP sheet on the transverse direction, a less "softened" behavior of concrete was observed, which caused an increase of the shear contribution from the concrete.
- Although the test results are limited, FRP-SMM has shown reasonably good prediction of the shear behavior of the FRP reinforced RC element. However, the authors are aware of the fact that the accuracy of the model should be verified with more shear tests by taking into account different parameters also. This will be accomplished at the next stage of the research effort by conducting further tests with the panel tester at the University of Houston.

ACKNOWLEDGMENTS

This research was supported by the National Science Foundation, award number 1100930. Steel bars used in this research were specially fabricated and donated by GERDAU AMERISTEEL Co. The FRP materials are donated by FYFE. Co. Their support is greatly acknowledged.

REFERENCES

Belarbi, A and Hsu, TTC. 1994. Constitutive Laws of Concrete in Tension and Reinforcing Bars Stiffened by Concrete. *ACI Structural Journal*, V. 91, No. 4, July-Aug., pp. 465-474.

Belarbi, A and Hsu, TTC. 1995. Constitutive Laws of Softened Concrete in Biaxial Tension Compression. *ACI Structural Journal*, V. 92, No. 5, Sept.-Oct., pp. 562-573.

Hsu, TTC, Belarbi, A, and Pang, XB. 1995. A Universal Panel Tester. *Journal of Testing and Evaluations*, ASTM, V. 23, No. 1, Jan., pp. 41-49.

Moslehy, Y. 2010. Constitutive Relationships and Smart Aggregates-based Damage Evaluation of FRP Retrofitted Concrete Membrane Elements. *Doctoral Thesis*, Department of Civil and Environmental Engineering, University of Houston.

Pang, XB, and Hsu, TTC. 1996. Fixed-Angle Softened-Truss Model for Reinforced Concrete. *ACI Structural Journal*, V. 93, No. 2, Mar.-Apr., pp. 197-207.

Vecchio, FJ, and Collins, MP. 1982. Response of Reinforced Concrete to In-Plane Shear and Normal Stresses. *Publication No. 82-03*, Department of Civil Engineering, University of Toronto, Mar. 1982, 332 pp.

Vecchio, FJ, and Collins, MP. 1986. The Modified Compression-Field Theory for Reinforced Concrete Elements subjected to shear. *ACI Structural Journal*, V. 83, No. 2, March-April., pp. 219-231.

Wang, J. 2006. Constitutive Relationships of Prestressed Concrete Membrane Elements. *Doctoral Thesis*, Department of Civil and Environmental Engineering, University of Houston.

Yang, G, Zomorodian, M, Belarbi A, Ayoub, AS, and Acun, B. 2013. Experimental and Analytical Investigations on the Behavior of FRP-Reinforced Concrete Element Subjected to Pure Shear. *Proceeding of 11th International Symposium on Fiber Reinforced Polymers For Reinforced Concrete Structures*, Guimarães, Portugal.

Zhang, LX, and Hsu, TTC. 1998. Behavior and Analysis of 100-MPa Concrete Membrane elements. *Journal of Structural Engineering*, ASCE, V. 124, No. 1, Jan., pp. 24-34.

Zhu, RRH, and Hsu, TTC. 2002. Poisson Effect in Reinforced Concrete Membrane Elements. *ACI Structural Journal*, V. 99, No. 5, Aug.-Sep., pp. 631-640.

Zomorodian, M, Yang, G, Belarbi A, Ayoub, AS, and Acun, B. 2013. Effects of Carbon Fiber Anchors on the Behavior of FRP Strengthened RC Elements Subjected to Pure Shear. *Proceeding of the Second Conference on Smart Monitoring, Assessment and Rehabilitation of Civil Structures*, Istanbul, Turkey.

NOTATIONS

A_c = area of the concrete
A_f = area of the FRP sheet
A_s = area of the steel
E_c = elastic modulus of concrete
E_f = elastic modulus of FRP sheet
E_s = elastic modulus of bare steel bars
f'_c = cylinder compressive strength of concrete
f_{cr} = cracking tensile strength of concrete
f_u = ultimate stress of FRP sheet
f_y = yield stress of bare steel bars
l = direction of longitudinal steel bars
t = direction of transverse steel bars
T_{frp} = thickness of the FRP sheet
α_1 = angle of applied principal tensile (1-axis) with respect to longitudinal steel bars (l-axis)
$\bar{\varepsilon}_1$ = smeared (average) strain in principal 1-direction when Hsu/Zhu ratios are considered
ε_{cr} = cracking tensile strain of concrete
ε_{fu} = ultimate strain in FRP sheet
σ_1^c = smeared (average) tensile stress of concrete in 1-direction
σ_2^c = smeared (average) compressive stress of concrete in 2-direction
σ_l = applied normal stress in l-direction of steel bars
σ_t = applied normal stress in t-direction of steel bars
τ_{12}^c = smeared (average) shear stress of concrete in 1-2 coordinate of applied stresses
τ_{lt} = applied shear stress in l-t coordinate of steel bars
ρ_f = FRP ratio
ρ_l = longitudinal steel ratio
ρ_t = transverse steel ratio
ζ_f = softened coefficient of concrete in compression when peak stress-softened coefficient is equal to strain-softened coefficient